Column studies to assess the effects of climate variables on redox processes during riverbank filtration

Matthias Rudolf von Rohr[1,2], Janet G. Hering[1,2,3], Hans-Peter E. Kohler[1,2], Urs von Gunten[1,2,3,*]

[1] EAWAG, Swiss Federal Institute of Aquatic Science and Technology, Water Resources & Drinking Water, Überlandstrasse 133, 8600 Dübendorf, Switzerland

[2] ETH Zürich, Institute of Biogeochemistry and Pollutant Dynamics, Universitätstrasse 16, 8092 Zürich, Switzerland

[3] Ecole Polytechnique Fédérale de Lausanne (EPFL), School of Architecture, Civil and Environmental Engineering (ENAC), 1015 Lausanne, Switzerland

*Corresponding author

Urs von Gunten

Überlandstrasse 133

P.O. Box 611

Phone: +41 58 765 5270

Fax: +41 58 765 5210

urs.vongunten@eawag.ch

Highlights

- Effects of climate variables on redox processes were tested in column studies
- Biodegradable dissolved organic matter was removed immediately at the column inlet
- Oxygen consumption was attributed to respiration of particulate organic matter
- Temperature and infiltration rate strongly affected the oxygen consumption
- Nitrate acted as a redox buffer preventing Mn(II) mobilization

Abstract

Riverbank filtration is an established technique used world-wide to produce clean drinking water in a reliable and cost-efficient way. This practice is, however, facing new challenges posed by climate change, as already observed during past heat waves with the local occurrence of anoxic conditions. In this study we investigated the effect of direct (temperature) and indirect (dissolved organic matter (DOM) concentration and composition, flow rate) climate change variables on redox processes (aerobic respiration, denitrification and Mn(III/IV)/Fe(III) reduction) by means of column experiments. Natural river water, modified river water and river water mixed with treated wastewater effluent were used as feed waters for the columns filled with natural sand from a river-infiltration system in Switzerland. Biodegradable dissolved organic matter was mainly removed immediately at the column inlet and particulate organic matter (POM) associated with the natural sand was the main electron donor for aerobic respiration throughout the column. Low infiltration rates (≤0.01 m/h) enhanced the oxygen consumption leading to anoxic conditions. DOM consumption did not seem to be sensitive to temperature, although oxygen consumption (i.e., associated with

53 POM degradation) showed a strong temperature dependence with an activation

54 energy of ~70 kJmol^{-1}. Anoxic conditions developed at 30°C with partial denitrification

55 and formation of nitrite and ammonium. In absence of oxygen and nitrate, Mn(II) was

56 mobilized at 20°C, highlighting the importance of nitrate acting as a redox buffer under

57 anoxic conditions preventing the reductive dissolution of Mn(III/IV)(hydr)oxides.

58 Reductive dissolution of Fe(III)(hydr)oxides was not observed under these conditions.

59

60 Keywords: climate change; redox milieu; microbial respiration; effluent ; POM; BDOM

61

1 Introduction

63 Several European countries rely on natural or engineered riverbank filtration to

64 produce drinking water, with a contribution of <~50% to the total drinking water

65 production in France (Hannappel et al., 2014), ~16% in Germany (Tufenkji et al., 2002)

66 and ~25% in Switzerland. During riverbank filtration, river water infiltrates through

67 riverbed sediments into an aquifer, from which it is extracted for drinking water

68 production. The derived groundwater often requires only minimal treatment before

69 distribution, because natural attenuation processes during infiltration efficiently remove

70 particles, microorganisms, natural organic matter (NOM) and partially remove organic

71 contaminants (Kuehn and Mueller, 2000; Grünheid et al., 2005; Schmidt et al., 2007;

72 Scheurer et al., 2012; Storck et al., 2012; Huntscha et al., 2013).

73   An important criteria for the quality of drinking water derived from riverbank

74 filtration is the redox milieu and the related geochemical processes. The redox milieu is

75 mainly determined by microbial respiration processes (redox processes), in which

76 NOM is the electron donor and oxygen, nitrate, Mn(III/IV)- and Fe(III)(hydr)oxides or

77   sulfate are the electron acceptors. These biogeochemical processes have been

78   extensively studied at riverbank filtration sites (Jacobs et al., 1988; Bourg and Bertin,

79   1993) and in laboratory column experiments (Matsunaga et al., 1993; von Gunten and

80   Zobrist, 1993). Seasonal changes in the redox milieu, in which anoxic (i.e. oxygen-

81   free) conditions develop and Mn(II) is mobilized in summer and aerobic conditions are

82   maintained in winter, have been ascribed to the temperature dependence of microbial

83   activity (von Gunten et al., 1991; Greskowiak et al., 2006; Massmann et al., 2006).

84   Besides temperature, the quantity and composition of NOM in river waters also

85   dictate the redox milieu during riverbank filtration, since NOM is an important substrate

86   for microbial respiration (Grünheid et al., 2005; Maeng et al., 2008). Previous studies

87   have focused on dissolved organic matter (DOM) as the main electron donor during

88   riverbank filtration (von Gunten and Zobrist, 1993; Grünheid et al., 2005; Grünheid et

89   al., 2008; Maeng et al., 2008). However, there is evidence that particulate organic

90   matter (POM) in the riverbed sediments may also contribute substantially as a

91   substrate to the consumption of electron acceptors (Grischek et al., 1998; Brugger et

92   al., 2001; Massmann et al., 2006; Diem et al., 2013b).

93   Furthermore, the hydraulic residence time, which is determined by the infiltration

94   rate, may influence the redox milieu during riverbank filtration. It is assumed that low

95   infiltration rates favor and high infiltration rates inhibit the formation of reducing

96   conditions in the aquifer (Doussan et al., 1997). Drought periods generally tend to

97   bring about anaerobic conditions during summer months as a consequence of long

98   residence times and high temperatures, whereas floods tend to increase the infiltration

99   rate and facilitate the breakthrough of pathogens, suspended solids and DOM

100   (Sprenger et al., 2011). Moreover, flood events can also lead to an increased oxygen

101   consumption in the infiltration zone, which has been attributed to an increased

102   deposition of POM in this zone under these conditions (Diem et al., 2013b).

103   All factors that dictate the redox milieu in the riverbank filtration zone may be

104   directly (temperature) or indirectly (NOM quantity and composition in river water,

105   residence time in the infiltration zone) influenced by climate and climate change. By

106   2085, average summer air temperatures in northern Switzerland are predicted to

107   increase by 4 K and average summer precipitation to decrease by 20% resulting in

108   lower discharges in rivers (CH2011, 2011; FOEN, 2012). The lower river discharges

109   may also lead to lower infiltration rates and thus longer hydraulic residence times in the

110   infiltration zone. In addition, decreasing natural flows will reduce the extent to which

111   effluent organic matter (EfOM) discharged from wastewater treatment plants is diluted

112   and consequently a higher proportion of EfOM in the receiving waters may be

113   expected. Better understanding of the effect of each climate factor on the redox milieu

114   will help to assess future changes in water quality during riverbank filtration.

115   We hypothesize that the direct and indirect effects of climate change will lead to

116   more frequent occurrence of anoxic conditions in riverbank filtration systems in the

117   future. This could create significant problems for drinking water supplies because of

118   the potentially more frequent occurrence of reduced species, such as nitrite, $Mn(II)$ and

119    $Fe(II)$. Nitrite is a toxic compound for which the WHO guideline is 900 µg N/L (WHO,

120   2011). When groundwater containing $Mn(II)$ and $Fe(II)$ is exposed to oxygen from the

121   air, the resulting precipitation of $Mn(III/IV)$- or $Fe(III)$(hydr)oxides can cause clogging of

122   filter screens and lead to rusty water and aesthetic problems (Mouchet, 1992; Hoehn

123   and Scholtis, 2011).

124   Here, we assess the effect of direct and indirect climate change variables on

125   redox conditions during riverbank filtration based on column experiments, in which

126   temperature, DOM concentration/composition and flow rate were systematically varied.

127   Moreover, the dynamics of the $Mn(II)$ and $Fe(II)$ mobilization under oxygen- and

128   nitrate-free conditions were investigated.

2 Materials and Methods

2.1 Set-up of the column system

Fig. S1 shows the set-up of the column system: Filtered Thur River water (0.45 µm, cellulose nitrate, Sartorius AG, Göttingen, Germany) was pumped from the bottom to the top of the column with a HPLC-pump (Jasco PU-2080, Jasco Corporation, Tokyo, Japan). The casing of the column consisted of a Plexiglas tube (length: 30 cm, inner diameter: 5.2 cm). The column was equipped with 13 sampling ports (SP1-13), in addition one was installed before (SP0) and one after (SP14) the column (Fig. S1). The column was packed with a dried sand fraction (grain size: 0.125-0.250 mm) sampled at a sand/gravel bar at the Thur River (Diem et al., 2013b). The relatively homogeneous sand fraction 0.125-0.250 mm contained 0.3 ± 0.2% (w/w, average of 12 sample aliquots) particulate organic carbon (POC). The filling procedure of the dry sand was conducted in form of a "sand rain", following von Gunten and Zobrist (1993). X-ray diffraction analysis of the sand showed mainly calcite and quartz (40% and 25%, respectively). Two columns (column I and II) filled with the same sand material were used for the respective experiments under different operational conditions (Section 2.2). We assessed the hydraulics in columns I and II by conducting tracer tests with a 8.55 mM NaCl solution. During the tracer tests, the electrical conductivity was measured at the end of the columns and was used for the calculation of the effective porosity and the dispersivity (Table 1).

River water was collected at Niederneunforn at a river-infiltration system of the peri-alpine Thur River, NE-Switzerland (Diem et al., 2013b), filtered and used as feed water from a 2 L storage tank (see Table S1 for chemical composition of all feed waters). The storage tank was replenished every three days with Thur River water stored at 5°C. For the experiments performed at 12.5°C, 20°C and 30°C, Thur River

154 water was equilibrated to the desired temperature before it was pumped into the

155 columns. No measurable DOM degradation (DOC concentration ± 0.1 mg C/L) was

156 observed in the storage tank under these conditions.

157   For varying operational conditions, the profiles of the oxygen concentration were

158 taken for steady-state conditions after an equilibration time of ≥20 d. Sampling was

159 conducted from the top to the bottom of the column in the opposite direction of the

160 water flow (Fig. S1). This procedure enabled sampling of fresh aliquots avoiding

161 sampling from stagnant zones. Oxygen and pH were directly measured at each

162 sampling port in a flow-through cell having a total dead volume of ~3 mL (Fig. S1). For

163 the analysis of DOC, major cations and anions, a 0.45 μm rinsed regenerated cellulose

164 filter (National Scientific Company, Rockwood, USA) was connected to the port of

165 interest and a ~40 mL sample was withdrawn for each sampling event (duration of

166 sampling: ~40 minutes at 1 mL/min). Oxygen, pH, DOC and nitrate were measured

167 between one and three times every 3-5 days (indicated in the figures by "n", i.e. the

168 number of measurement replicates). For Fe and Mn analysis, a 9 mL sample was

169 acidified to pH 2 with 1 mL of 1 M HCl.

170

171 (Table 1)

172

173 2.2 Operational conditions of the column experiments

174 Six different column experiments with varying parameters (feed water, temperature,

175 flow rate) were conducted either with column I or II (Table 2). The first experiments for

176 each column (experiment 1.1 for column I and experiment 2.1 for column II,

177 respectively) were initiated after an equilibration time of 2 months feeding Thur River

178 water to reach steady-state conditions for oxygen and DOC.

179   For experiment 1.1, treated wastewater effluent (herein simply named effluent)

180   from a municipal wastewater treatment plant (Dübendorf Neugut, Switzerland) was first

181   filtered (0.45 µm, cellulose nitrate, Sartorius AG, Göttingen, Germany). The filtered

182   effluent was then electrodialysed (PCCell GmbH, Heusweiler, Germany) to remove

183   nitrate prior to preparing four Thur River water/effluent mixtures to be used as feed

184   waters (Tables S1 and S2) to study the effect of the type and concentration of DOM on

185   the oxygen consumption.

186   In experiment 1.2, the effect of the flow rate on the oxygen consumption was

187   investigated. Four flow rates, simulating different infiltration velocities, were chosen:

188   0.1, 0.2, 0.33 and 1.0 mL/min.

189   In experiment 2.1, the temperature dependence of the oxygen consumption and

190   NOM degradation was investigated at four temperatures (5, 12.5, 20 and 30°C). While

191   the experiments at 5.0, 12.5 and 20.0°C were carried out with the storage tank at

192   ambient laboratory temperature (22 ± 2°C), for the 30.0°C experiment the tank had to

193   be placed inside the incubator to prevent outgassing in the HPLC-pump.

194   In experiment 2.2, unaltered Thur River water was added as feed water and in

195   experiment 2.3, "DOM-free" Thur River water was used as feed water to study the

196   effect of POM on the oxygen consumption. About 96% of the DOM was removed from

197   the Thur River water by addition of 500 mg/L Norit W15 powdered activated carbon

198   (NORIT Deutschland GmbH, Riesbürg, Germany) and filtration through a 0.45 µm filter

199   (cellulose nitrate, Sartorius AG, Göttingen, Germany). DOM removal was achieved

200   without significantly affecting the other water quality parameters (Table S3).

201   In experiment 2.4, a readily available DOM source in form of sodium acetate (6

202   mg/L or 1.75 mg C/L) was added to the Thur River water inflow immediately before the

203   column inlet (at sampling port SP0) to investigate the effect of easily biodegradable

204   DOM (BDOM) on the oxygen consumption.

205   In experiment 2.5, the dynamics of the Mn(II) and Fe(II) mobilization under

206   oxygen- and nitrate-free conditions were investigated. Thur River water was

207   electrodialysed to remove nitrate and was re-mineralized thereafter to obtain a similar

208   water composition as the original river water with respect to the alkalinity and the major

209   cations and anions (Table S4). To remove oxygen from the feed water, it was

210   continuously purged with a N_2/CO_2 gas mixture (99.96% N_2 / 0.04% CO_2) leading to an

211   oxygen concentration below 0.1 mg/L at SP0.

212   All column experiments except 1.1 and 1.2 were conducted in an incubator (±

213   1°C). Column experiment 1.1 was carried out at ambient laboratory temperature (22 ±

214   2°C) and experiment 1.2 in a climatised chamber (20 ± 1°C). Column I was operated

215   aerobically (experiments 1.1 and 1.2), whereas column II was first operated aerobically

216   for 327 days (experiments 2.1, 2.2, 2.3 and 2.4) and then anaerobically for 66 days

217   (experiment 2.5).

218

219   (Table 2)

220

221   2.3 Analytical methods

222   Oxygen and temperature were measured with an optical sensor LDO101 (Hach Lange

223   GmbH, Berlin, Germany, limit of quantification 0.1 mg/L, accuracy ± 0.1 mg/L, T ± 0.3

224   K), pH was measured with a pH electrode PHC 301 (Hach Lange GmbH, Berlin,

225   Germany, accuracy pH ± 0.1). DOC was taken as a measure for DOM and was

226   determined by catalytic combustion at 720°C with a Shimadzu TOC-V CPH analyzer

227   (Shimadzu Corporation, Kyoto, Japan). The limit of quantification was 0.1 mg C/L and

228   the error of measurement ± 0.1 mg C/L. The alkalinity was determined with a Metrohm

229   809 Titrando (Metrohm Schweiz AG, Zofingen, Switzerland). NO_2^- and NH_4^+ were

230   analyzed photometrically with a spectrophotometer Cary 100 Scan Spectrophotometer

231 (Varian AG, Zug, Switzerland) following the norms EN 26777 (DIN, 1993) and DIN

232 38406 (DIN, 1983a), respectively. The limit of quantification was 0.01 mg N/L and the

233 error of measurement ± 0.002 mg N/L for both compounds. PO_4^{3-} was measured with

234 a spectrophotometer Varian Cary 50 Bio (Varian AG, Zug, Switzerland) according to

235 Vogler (1965). NO_3^-, Cl^-, SO_4^{2-}, Na^+, K^+, Ca^{2+} and Mg^{2+} were analyzed with a Metrohm

236 761 Compact IC (Metrohm Schweiz AG, Zofingen, Switzerland) using a "Metrohm

237 Metrosep A Supp 5 100/4 mm" column for the anions and a "Metrohm Cation 1-2 125/4

238 mm" column for the cations. For NO_3^-, the limit of quantification was 0.25 mg N/L and

239 the error of measurement ± 0.1 mg N/L. NO_3^- concentrations <0.25 mg N/L (i.e. for the

240 preparation of the oxygen- and nitrate-free Thur River water, experiment 2.5), were

241 measured with a spectrophotometer Varian Cary 50 Bio (Varian AG, Zug, Switzerland)

242 according to Müller and Widemann (1955). Here, the limit of quantification was 0.1 mg

243 N/L and the error of measurement ± 0.02 mg N/L. Fe and Mn were measured with

244 inductively coupled plasma atomic emission spectroscopy (ICP-OES) as total Fe and

245 total Mn concentrations, respectively (SPECTRO Analytical Instruments GmbH, Kleve,

246 Germany). The limit of quantification was 0.1 µg/L and the error of measurement ± 0.1

247 µg/L. It could be shown that total Mn corresponded to Mn(II) measured colorimetrically

248 (DIN, 1983b).

249 The POC concentration of the column sand representing POM was determined

250 by subtracting the content of inorganic carbon, measured with a CO_2 Coulometer

251 CM5015 (UIC Inc., Joilet, USA), from the total carbon, measured with a CNS analyzer

252 Eurovector EA3000 (Hekatech GmbH, Wegberg, Germany).

253 A closed bottle biological oxygen demand (BOD) test of the natural sand was

254 conducted by BMG Engineering Ltd., Schlieren, Switzerland as a batch experiment by

255 incubating the sand (3.2 g/L) with an inoculum of a secondary effluent from a municipal

256 wastewater treatment plant at 22°C and measuring the decrease in the oxygen

257   concentration (OECD, 1992). Five batch experiments with different duration were

258   conducted (5, 7, 14, 21 and 28 days). Each batch experiment was done in duplicate

259   (indicated by "n=2").

260   The protein content of the pristine sand and of the sand samples from column II

261   was measured according to the bicinchoninic acid method using an assay-kit of Sigma-

262   Aldrich (Smith et al., 1985) after protein extraction with 1 M NaOH at 95°C for 30

263   minutes (Herbert et al., 1971). Three samples were withdrawn from column II for each

264   sampling port of interest (indicated by "n=3") after 393 days of operation (i.e., at the

265   end of experiment 2.5). The pristine sand was washed with nanopure water before

266   protein measurements to determine the blank protein content.

267   The quantification of the reactive pool of Mn(III/IV)(hydr)oxides of the pristine

268   and of the column II sand was conducted at the end of experiment 2.5 with a buffered

269   ascorbate solution according to Hyacinthe et al. (2006). Samples were withdrawn from

270   column II at SP1, SP5, SP8, SP11 and SP13 using a specially designed "sand scoop".

271   2.6 g of each sample was mixed with a 150 mL solution consisting of sodium citrate

272   (50 g/L), sodium bicarbonate (50 g/L) and L(+) ascorbic acid (20 g/L) (pH 7.1), which

273   was continuously purged with N_2. The experiment was conducted for 2.5 hours and

274   samples were taken after 0.5, 1, and 2.5 hours for ICP-OES analysis.

275 2.4 Calculation of manganese concentration in equilibrium with $MnCO_3$

276 The Mn^{2+} concentration in equilibrium with $MnCO_3$ was calculated based on the

277 solubility product of rhodochrosite ($MnCO_3$) ($Mn^{2+} + CO_3^{2-} = MnCO_3$; log K = -10.39

278 (Stumm and Morgan, 1996)) and on the CO_3^{2-} concentration of 3.34×10^{-5} M. The latter

279 value was calculated from the measured concentration of HCO_3^- and pH (8.2) in the

280 column during experiment 2.5. The total Mn(II) concentration was then derived by

281 inserting the calculated Mn^{2+} equilibrium concentration, the measured calcium and

282 HCO_3^- concentrations and the pH in the chemical equilibrium modeling program

283 ChemEQL V3.0 (Mueller, 2004). The resulting Mn(II) speciation is shown in Table S5.

284 The sum of all relevant Mn(II) species is shown as equilibrium concentration (Fig. S2

285 (dashed line)).

286

287 **3 Results and discussion**

288 3.1 Effect of indirect climate change variables on redox processes

289 *3.1.1 Oxygen and pH profiles*

290 We investigated the effects of increasing DOC concentration and altered DOM

291 composition on redox processes by utilizing varying mixtures of Thur River water and

292 effluent (experiment 1.1), "DOM-free" Thur River water (experiment 2.3) and Thur

293 River water amended with acetate (experiment 2.4) as feed waters. All oxygen profiles

294 showed a fast initial decrease of the relative oxygen concentration, which is discussed

295 later (see Section 3.1.3), followed by a slower decrease between SP1 and SP14 (Fig.

296 1a). The residence times in Fig. 1a and 1b were calculated by dividing the pore volume

297 at a specific sampling port by the flow rate of the respective experiment. The pH

298 dropped in parallel to the fast initial oxygen drop close to the inlet and showed a slower

299 decrease thereafter (Fig. 1b). Both the oxygen and pH profiles can be explained by

300 aerobic respiration (Eq. 1). The decrease of the pH, which was caused by formation of

301 CO_2, was only partially prevented by the buffering capacity of calcium/magnesium

302 carbonates.

303

304 $$CH_2O + O_2 \, (aq) \rightarrow CO_2 \, (aq) + H_2O \qquad \qquad (1)$$

305
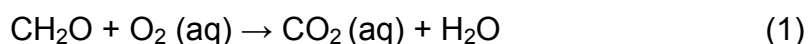
306 In Eq. 1, CH_2O represents DOM with carbon in a zero-valent oxidation state.

307

308 (Fig. 1)

309

310 *3.1.2 Role of wastewater effluent and particulate organic matter (POM)*

311 The addition of effluent of up to 40% (experiment 1.1) did not enhance the oxygen

312 consumption in the column (Fig. 1a) even though the DOC concentration was

313 increased by up to 1.4 mg C/L compared with the unamended (experiment 2.2) Thur

314 River water (see Table S1). The profile of the relative oxygen concentration of the

315 "DOM-free" Thur River water (experiment 2.3) showed a similar decreasing trend

316 between SP1 and SP14 as the original Thur River water (Fig. 1a). This means that the

317 oxygen consumption did not depend on the presence of DOM in the feed water. Thur

318 River water contains mostly humic compounds that are rather persistent (Peter et al.,

319 2012). However, other river waters might contain significantly higher concentrations of

320 biodegradable DOM, which could affect the oxygen consumption during riverbank

321 filtration.

322   Based on our results, we hypothesize that the electron donor is associated with

323 the sand matrix and consists of particulate organic matter (POM). Our results are in

324 line with previous column studies conducted with river water (DOC concentration of 15

325   mg C/L) and a river water/effluent mixture (50% effluent, DOC concentration of 17 mg

326   C/L) showing no enhanced oxygen consumption with the addition of a river

327   water/effluent mixture (Maeng et al., 2008). Furthermore, it has been suggested in field

328   investigations that POM is likely to act as an important electron donor during riverbank

329   filtration (Grischek et al., 1998; Brugger et al., 2001; Massmann et al., 2006; Kedziorek

330   et al., 2008; Diem et al., 2013b). These previous studies have based their conclusions

331   on mass balance calculations of experimental field data. Here, we provide independent

332   evidence from controlled laboratory experiments to support these field observations.

333   To investigate the role of POM associated with the sand as a support for aerobic

334   respiration in the column, a biological oxygen demand (BOD) test of the pristine sand

335   was conducted. Fig. 2 shows the BOD of the sand determined after 5, 7, 14, 21 and 28

336   days. Even after 28 days, the BOD had not reached a plateau; the maximum observed

337   value was ~9 x 10^{-4} mg O_2/mg sand corresponding to a total BOD of at least 800 mg

338   O_2 for the entire sand columns. If we consider that 7 mg/L oxygen was consumed on

339   average in the column with the original Thur River water as feed water based on

340   oxygen saturation conditions at SP0 (Fig. 1a), then ~3 mg O_2 will be consumed per

341   day. The available POM could therefore sustain aerobic respiration for at least 260

342   days without being exhausted.

343

344   (Fig. 2)

345

346   *3.1.3 Role of easily biodegradable DOM (BDOM)*

347   The addition of acetate (1.75 mg C/L, ~0.14 mM C) led to an increased oxygen

348   consumption between the first two sampling ports (Fig. 1a). The "theoretical" oxygen

349   consumption assuming complete mineralization of the added acetate and steady-state

350   conditions with respect to DOM sorption and desorption processes (Sobczak and

351   Findlay, 2002), is ~4.7 mg/L O_2 (~0.14 mM) ($CH_3COOH + 2O_2 \rightarrow 2CO_2 + 2H_2O$). This

352   value is in good agreement with the measured oxygen consumption of 4.2 mg/L

353   between the first two sampling ports. Therefore, this suggests that the fast initial

354   oxygen decrease is attributed to the mineralization of acetate, as a model for BDOM,

355   which implies that acetate and not POM was preferentially consumed at the column

356   inlet under these conditions.

357   Previous results have shown that the addition of a readily available carbon

358   source, such as lactic acid (14 mg C/L), led to a complete consumption of oxygen

359   within the first 1.8 cm of a 30 cm column (von Gunten and Zobrist, 1993). The authors

360   of this study also showed that the highest rate of the oxygen consumption occurred at

361   the column inlet and was attributed to a higher microbial activity in this zone supported

362   by a higher BDOM availability, as also demonstrated by Maeng et al. (2008).

363   For all experiments except for acetate addition, a similar fast initial decrease of

364   the oxygen concentration between SP0 and SP1 could be observed (Fig. 1a). This

365   decrease cannot be totally explained by BDOM degradation, since the differences in

366   DOC concentrations for the Thur River water and Thur/effluent mixtures were small

367   (<0.2 mg C/L) and below the limit of quantification for the "DOM-free" experiment.

368   Small BDOM levels in the Thur River water could however have served as a substrate

369   to stimulate bacterial growth leading to higher bacterial concentrations in this zone

370   (see Section 3.2.2) allowing for a higher oxygen consumption rate associated with

371   POM degradation.

372

373   *3.1.4 Effect of flow rate*

374   To assess the dependence of the oxygen consumption and NOM degradation on the

375   flow rate, four experiments under different flow rate conditions (0.1, 0.2, 0.33 and

376   1 mL/min, i.e. residence times of 40, 20, 12 and 4 hours, respectively) were conducted

377   at 20°C. The profiles of the relative oxygen concentration depended on the flow rate if

378   plotted as function of the infiltration distance (Fig. 3a), please note normalization to

379   SP1). At the highest flow rate of 1 mL/min, oxic conditions persisted through the entire

380   column, whereas at the flow rate of 0.2 mL/min (i.e. 0.01 m/h), anoxic conditions could

381   be observed within 20 cm of the column inlet (Fig. 3a). Lower flow rates increased the

382   hydraulic residence time allowing for a higher oxygen consumption in the same zone of

383   the column and leading to anoxic conditions, which is in agreement with Doussan et al.

384   (1997). Fig. 3b shows that the oxygen concentrations curves are superimposable when

385   plotted against the hydraulic residence time, indicating that the differences in the

386   residence times fully account for the observed effects of flow rate.

387

388   (Fig. 3)

389

390   3.2 Effect of direct climate change variable (temperature) on redox processes

391   *3.2.1 Electron balance for oxygen consumption and NOM degradation*

392   The influence of temperature on the oxygen consumption and on NOM degradation

393   was investigated in four column experiments conducted with Thur River water at 5.0,

394   12.5, 20.0 and 30.0°C. The oxygen and DOM consumption (measured as difference in

395   DOC concentration) between the column inlet and outlet is shown as a function of

396   temperature in Fig. 4. The DOM consumption between the column inlet and outlet

397   explained only ~30% of the oxygen consumption at 5°C and <~7% at 12.5°C-30°C. At

398   30°C, the DOM consumption was lower than at the other temperatures possibly

399   because of partial DOM degradation (~0.1 mg C/L, i.e. ~8 mM) already in the storage

400   tank. The small contributions of the DOM consumption to the oxygen consumption for

401   each temperature are a further confirmation for the hypothesis that POM associated

402   with the sand is most likely the electron donor for aerobic respiration (see Section

403   3.1.2).

404   A strong temperature dependence of the oxygen consumption could be

405   observed between the column inlet and outlet reaching almost a plateau at 20°C (Fig.

406   4, white bars). Conversely, the DOM consumption between the column inlet and outlet

407   did not seem to depend on temperature, since the values lie within the measurement

408   uncertainty (Fig. 4, grey bars).

409   The small DOM consumption (<17 µM C, i.e. 0.2 mg C/L) between the column

410   inlet and outlet for all temperatures could be related to the recalcitrant nature of the

411   DOM. Previous results from column studies also did not show any temperature

412   dependence of the DOM consumption after the first sampling point at a retention time

413   of about one day (Grünheid et al., 2008). Moreover, the authors of field studies at river-

414   infiltration systems observed a high correlation between oxygen consumption and

415   temperature, but no correlation between DOM consumption and temperature (Brugger

416   et al., 2001; Diem et al., 2013b).

417

418   (Fig. 4)

419

420   *3.2.2 Kinetics of oxygen consumption*

421   The measured oxygen concentration profiles for each temperature (5°C, 12.5°C, 20°C

422   and 30°C) are shown in Fig. 5. The oxygen concentration of the feed water was 7.8

423   mg/L at 5.0°C, 12.5°C and 20.0°C and 7.0 mg/L at 30.0°C. Similarly to the previous

424   experiments (see Section 3.1.1), the highest rates of the oxygen consumption could be

425   observed at the column inlet (i.e., between SP0 and SP1) (Fig. 5).

426

427   (Fig. 5)

428

429   After the initial phase, the profiles of the oxygen concentration showed a nearly

430   linear behavior, corresponding to zero-order kinetics (Fig. 5). This can be normally

431   observed when the rate at which the growth-limiting nutrient becomes available is the

432   rate-limiting step (Alexander, 1999). In our case, POM is assumed to be the primary

433   electron donor for microbial respiration and hence for oxygen consumption. POM

434   degradation involves hydrolytic reactions (Egli, 1995; Pusch et al., 1998) generating

435   BDOM, which is subsequently oxidized to CO_2 by aerobic respiration. Fig. 6 shows a

436   schematic representation of the processes involving POM hydrolysis (reaction 1) and

437   BDOM oxidation (reaction 2), respectively. Oxygen and CO_2 in the aqueous solution

438   enter the biofilm through diffusion. The hydrolytic reactions are commonly assumed to

439   be the rate-limiting step for POM degradation (Valentini et al., 1997; Henze et al.,

440   1999; Vavilin et al., 2008). Therefore, we hypothesize that the observed oxygen

441   consumption rates for each temperature were mainly controlled by POM hydrolysis.

442   This, together with the large POM reservoir identified in the column sand through the

443   BOD measurements, explains well the observed pseudo-zero order reaction kinetics

444   for the oxygen consumption in the column.

445

446   (Fig. 6)

447

448   The observed pseudo-zero order behavior also implies that the concentration of

449   bacteria must be fairly constant over the length of the column (between SP1 and

450   SP13). Bacterial densities were estimated indirectly by a protein assay conducted at

451   the end of experiment 2.5 after column II was operated anaerobically for 66 days (see

452   Section 2.3 for analytical methods). We expect that the protein content of the sand

453   samples from column II did not vary significantly after having changed the column

454   operation mode from aerobic, which lasted 327 days, to anaerobic (66 days).

455   The protein content of the pristine sand was lower than the samples from the

456   column, indicating that a significant bacterial growth occurred during the column

457   experiments (Fig. 7). Nearly constant protein concentrations were measured in

458   samples SP2-SP13 suggesting a uniform growth and distribution of bacteria through

459   the column (Fig. 7). This implies that POM supporting bacterial growth was hydrolyzed

460   at a constant rate throughout the column (i.e., after SP1), which is consistent with the

461   observed pseudo-zero order reaction kinetics for the oxygen consumption. A higher

462   protein concentration in sample SP1 compared with the average of SP2-SP13 (p

463   <0.001, Z-test statistics) may reflect bacterial growth by the presence of non-

464   measurable BDOM near the column inlet (see Section 3.1.3).

465

466   (Fig. 7)

467

468   *3.2.3 Temperature dependence of aerobic respiration: Activation energy*

469   The oxygen consumption in the column has been shown to be associated with the

470   degradation of POM present on the sand and to depend on temperature (Fig. 5). To

471   quantify the observed temperature dependence, an Arrhenius-type approach, typical

472   for chemical and biological reactions (Middelburg et al., 1996; Weston and Joye, 2005;

473   Burdige, 2011), was applied (Eq. 2):

474
$$\ln(k(T)) = \ln(A) - \frac{E_a}{R} \cdot \frac{1}{T} \qquad (2)$$

475   where $k(T)$ is the temperature-dependent reaction rate constant (in our case the

476   observed pseudo zero-order oxygen consumption rate constant in Ms^{-1}), A the pre-

477   exponential factor (in Ms^{-1}), E_a the apparent Arrhenius activation energy (in $Jmol^{-1}$), R

478   the universal gas constant (in $Jmol^{-1}K^{-1}$) and T the temperature (in K). Fig. 8 shows an

479   Arrhenius-type plot of the data. Based on the good linearity (r^2=0.97), the apparent

480   activation energy E_a can be determined from the slope $\left(\dfrac{E_a}{R}\right)$ of the straight line in Fig.

481   8, which results in a value of ~70 $kJmol^{-1}$.

482

483   (Fig. 8)

484

485   The E_a value of ~70 $kJmol^{-1}$ derived from our column experiments is consistent

486   with a value of 51 ± 12 $kJmol^{-1}$ (n=94) determined from measurements of benthic

487   respiration over the temperature range 5-25°C on stones collected from the Thur River

488   (Acuna et al., 2008). Similar values of 54-125 $kJmol^{-1}$ (Middelburg et al., 1996) and 46-

489   89 $kJmol^{-1}$ (Weston and Joye, 2005) were reported in studies of the temperature

490   dependence of organic matter degradation in intertidal and marine sediments,

491   respectively.

492   The activation energy for oxygen consumption can also be calculated from field

493   observations of oxygen concentrations at, for example, the Thur River infiltration

494   system (Diem et al., 2013a). In this study, the oxygen consumption rates were

495   modeled with a temperature factor defined by a function with a maximum rate at 35°C

496   (O'Connell, 1990) and with a discharge-dependent term. The activation energy for

497   aerobic respiration during infiltration was estimated to be ~63 $kJmol^{-1}$ over the

498   temperature range 5-30°C for low river discharges of <20 m^3/s (Diem et al., 2013a).

499   This activation energy is similar to our experimentally derived activation energy (~70

500    $kJmol^{-1}$), showing a good agreement between the field-based model and our

501   experimentally derived value.

502

503　*3.2.4 Redox processes involving nitrogen species*

504　The profiles of the oxygen concentration in Fig. 5 show that the oxygen consumption

505　rate increased with increasing temperatures, leading to anoxic conditions at 30.0°C for

506　residence times >7 h (i.e., at SP11, after 18 cm). To better characterize the redox

507　milieu under such conditions, nitrate, nitrite and ammonium were measured in the

508　column after an operation time of 18 days (Fig. 9). As soon as the oxygen

509　concentration approached ≤0.1 mg/L, nitrite started to increase, reaching a maximum

510　of 55 µg N/L at a residence time of about 10 h (Fig. 9). Ammonium appeared at a

511　residence time of about 8 h and did not reach a maximum. Nitrate showed a

512　decreasing trend for residence times >8 h (i.e., at SP12, after 22 cm). These findings

513　indicate that denitrification proceeded in the same section of the column where nitrite,

514　an intermediate product of denitrification, was formed. This view was corroborated by

515　the fact that ~30% of the nitrate decrease can be explained by the detected nitrite

516　concentration. The remaining 70% of the nitrate lost might be explained by the

517　formation of N_2, or other denitrification products (e.g. N_2O). Formation of ammonium

518　could be related to the anoxic degradation of nitrogen containing organic compounds,

519　or to nitrate ammonification. The maximum detected nitrite concentration (55 µg N/L) is

520　about one order of magnitude lower than the concentration recommended in the WHO

521　guideline for drinking water (900 µg N/L) (WHO, 2011) and in a similar range as the

522　value in the European guideline (150 µg N/L) (EU, 1998). Although the nitrite

523　concentrations given in the WHO and EU guidelines are not exceeded under our

524　experimental conditions, the formation of nitrite represents a potential threat for

525　drinking water quality under such anoxic conditions.

526

527　(Fig. 9)

528

529 3.3 Mobilization of Mn(II) under oxygen- and nitrate-free conditions

530 Nitrate-free Thur River water stripped of oxygen was added as feed water to test

531 whether Mn(III/IV)- and Fe(III)-reducing conditions could develop under this scenario.

532 No Fe(II) could be measured in the entire column during this experiment, whereas Mn

533 was mobilized as Mn(II) (Fig. 10a), suggesting that in the absence of oxygen and

534 nitrate, Mn(III/IV)(hydr)oxides became terminal electron acceptors for the

535 microorganisms.

536 According to the homogeneous POM distribution throughout the column and in

537 analogy to aerobic respiration, we would have expected a constant reductive

538 dissolution rate of Mn(III/IV)(hydr)oxides throughout the column leading to a steady

539 Mn(II) increase between SP1-SP14, only limited by $MnCO_3$ solubility (for calculations,

540 see Section 2.4). However, we observed a fast increase of Mn(II) near the column inlet

541 (SP1-SP5) after 9, 16 and 27 days, followed by a decrease beyond SP8 (Fig. S2). This

542 can also be observed in Fig. 10a, which shows the Mn(II) concentration as a function

543 of the column operation time for each sampling port. Here, the Mn(II) concentration

544 increased quickly for all sampling ports and peaked after ~7, ~14 and ~21 days for

545 SP1, SP5 and SP8, respectively, approaching zero after that, whereas it reached

546 $MnCO_3$ equilibrium for SP11 and SP14 (Fig. 10a).

547 We hypothesize that the fast Mn increase near the column inlet could be

548 associated with a higher biological activity in this zone (see Section 3.2.2) and hence

549 to a higher POM hydrolysis rate. From the experiments under aerobic conditions at

550 20°C (Fig. 1a and Fig. 5), we already observed a fast oxygen consumption at the

551 column inlet (SP0-SP1) related to POM hydrolysis generating BDOM. In absence of

552 oxygen and nitrate, part of this BDOM could propagate into the column and be

553 available for Mn(III/IV) reduction. The decrease of the Mn(II) concentration beyond

22

554 SP8 (Fig. S2) could be due to adsorption processes of Mn(II) on e.g.,

555 Mn(III/IV)(hydr)oxide surfaces.

556   Furthermore, the Mn(II) concentration profiles in Fig. S2 are shifted towards the

557 outlet with increasing operation time, possibly because of a depletion of

558 Mn(III/IV)(hydr)oxides in the zone between SP1-SP8. To test this hypothesis, the

559 reactive pools of Mn(III/IV)(hydr)oxides of the pristine and the column sand were

560 quantified at the end of the experiment (after 66 days) with a buffered ascorbate

561 solution at pH 7.1, according to Hyacinthe et al. (2006) (see Section 2.3). The amount

562 of Mn(II) reduced by ascorbate in the pristine sand (~23 µg/g sand) was significantly

563 higher than that in the column sand for all sampling ports, showing that a considerable

564 part of the reactive Mn pool was consumed during the experiment (Fig. 10b). Lower

565 Mn(II) sand concentrations were found at SP1 and SP5 compared to SP8, SP11 and

566 SP14 (Fig. 10b). This is a confirmation of a partial depletion of the reactive pool of

567 Mn(III/IV)(hydr)oxides at SP1 and SP5.

568   As a consequence of the initial depletion of the Mn pool, the extent of reductive

569 dissolution rate of Mn(III/IV)(hydr)oxides decreased in the first section of the column

570 (SP1-SP5) with increasing column operation time. This led to lower Mn(II)

571 concentrations at SP1, SP5 and possibly SP8 (the Mn(II) concentration at SP8 reflects

572 the accumulation of Mn(II) between SP1-SP8). For the sampling ports further in the

573 column (SP8, SP11 and SP14), higher manganese concentrations in the sand were

574 found (Fig. 10b), giving sufficient potential for a further increase of Mn(II) at SP11 and

575 SP14. However, the Mn(II) concentrations at these sampling points were limited by the

576 solubility of $MnCO_3$.

577   Even though ~75 µg Fe/g sand could be measured in the pristine sand by the

578 ascorbate method (data not shown), Fe(II) could not be detected during the

579 experiment. This suggests that conditions favorable for the reductive dissolution of

580 Fe(III)(hydr)oxides did not occur in our experimental system, but cannot be excluded at

581 actual riverbank filtrations sites.

582

583 (Fig. 10)

584

585 3.4 Practical implications

586 Several studies have investigated the impact of climate change on groundwater

587 quantity, but only a few have focused on processes affecting groundwater quality

588 (Green et al., 2011). A recent review by Sprenger et al. (2011) evaluated the

589 vulnerability of riverbank filtration systems to climate change considering two

590 scenarios, drought and flood. Overall, increasing surface water temperatures are

591 expected to favor anoxic/anaerobic conditions in the future (Sprenger et al., 2011),

592 which is in line with our results (see Sections 3.2.2 and 3.2.4). High vulnerability for the

593 drought scenario is projected for the DOM removal because of higher DOC

594 concentrations in the source water and incomplete degradation under anaerobic

595 conditions (Sprenger et al., 2011). The effects of the presumed increased DOC

596 concentrations and altered DOM composition on the redox processes are however still

597 unknown.

598   Currently, an upgrade of wastewater treatment plant effluents in Switzerland

599 with ozonation (Joss et al., 2008; Zimmermann et al., 2011) or powdered activated

600 carbon (Nowotny et al., 2007) is planned to reduce the discharge of organic

601 micropollutants to the water bodies. Ozonation is usually followed by a sand filtration

602 step, which effectively removes BDOM formed during ozonation (Zimmermann et al.,

603 2011). Powdered activated carbon treatment reduces DOM by adsorption processes

604 (Nowotny et al., 2007; Worch, 2010). Therefore, DOM loads from upgraded

605 wastewater treatment plants into the receiving rivers are expected to be reduced in the

606 future, counteracting the smaller dilution, which would lead to higher DOC

607 concentrations. In addition to that, our results showed that increasing DOC

608 concentrations from wastewater effluent did not affect the redox processes in our

609 experimental system (see Section 3.1.2). Based on the lower DOM input in rivers by

610 polishing treatment of wastewater plant effluents and its subordinate role as an

611 electron donor, only a minor effect of DOM on the development of anoxic conditions is

612 expected during future summer conditions.

613   In the column experiments, a significant effect of the hydraulic residence time on

614 the oxygen consumption and on the development of anoxic conditions was observed

615 (see Section 3.1.4). At the same time, however, high hydraulic residence times are

616 beneficial for the removal of microorganisms and pathogens (Sprenger et al., 2011).

617 Since infectious diseases represent the most important health risks with respect to

618 drinking water, removal of microorganisms and pathogens has absolute priority (WHO,

619 2011). The Swiss regulation for groundwater protection defines a minimum

620 groundwater travel time of 10 days before abstraction, which allows for an adequate

621 inactivation of microorganisms (Kunz et al., 2009). To determine the optimal residence

622 time, which allows for good pathogen removal without the formation of anoxic

623 conditions, site-specific information about the hydrogeological conditions and the redox

624 parameters are needed, as also suggested by Schoenheinz and Grischek (2011).

625   Today, groundwater derived from riverbank filtration in Switzerland is generally

626 oxic and denitrification is rarely observed. During future summer conditions, however,

627 the effect of high temperatures ($\geq 20°C$) over several weeks/months could lead to

628 transient anoxic conditions. Complete denitrification was not observed in the present

629 study, but cannot be excluded at actual riverbank filtration systems during future heat

630 waves. Therefore, it will be essential to monitor oxygen and nitrogen species (nitrate,

631   nitrite and ammonium) at riverbank filtration systems especially during future heat

632   waves.

633   The formation of ammonium could be problematic in the context of drinking

634   water disinfection, since it can quickly react with chlorine leading to the formation of

635   chloramines ($HOCl + NH_3 \rightarrow NH_2Cl + H_2O$), which lower the disinfection efficiency

636   (Deborde and von Gunten, 2008). At Swiss riverbank filtration systems, such as the

637   Thur River, disinfection is not practiced, but in cases where low chlorine doses are

638   applied (e.g. 7 µM Cl_2 or 0.5 mg/L Cl_2), the formation of ammonium in moderate

639   concentrations (<7 µM NH_4^+) can substantially reduce the disinfection efficiency of

640   chlorine.

641

642   4 Conclusion

643   Laboratory column experiments carried out with filtered river water were conducted to

644   simulate the effect of temperature, DOM concentration/composition and flow rate on

645   redox processes during riverbank filtration. The following conclusions can be drawn

646   from our results:

647   1. Biodegradable dissolved organic matter (BDOM) was mainly removed immediately

648   at the column inlet by aerobic respiration. This might lead to higher microbial

649   concentrations near the infiltration zone at actual riverbank filtration systems even if

650   BDOM is not measurable. DOM from wastewater treatment plant effluents did not

651   enhance aerobic respiration and did not promote anoxic conditions in our laboratory

652   columns.

653   2. Particulate organic matter (POM) associated with natural sand appears to be the

654   main terminal electron donor in the infiltration process and can sustain aerobic

26

655 respiration for long periods. A POM limitation was not observed in the laboratory

656 column system.

657 3. Low infiltration rates induce a higher oxygen consumption than higher rates for a

658 certain infiltration distance, which could lead to anoxic conditions.

659 4. The aerobic respiration associated with POM degradation strongly depends on

660 temperature with an activation energy of ~70 kJmol^{-1}. Only a small fraction of the

661 riverine DOM is easily degradable (i.e., BDOM) and its consumption does not seem to

662 be sensitive to temperature.

663 5. At high temperatures (30°C), fully anoxic conditions were observed, with partial

664 denitrification (~30%) and formation of nitrite and ammonium. Although nitrite

665 concentrations were below WHO and EU drinking water guidelines in our experiments,

666 this parameter should be monitored at actual riverbank filtration sites during future heat

667 waves. If the produced water is chlorinated, the presence of ammonium could lead to a

668 reduction in disinfection efficiency due to chloramine formation.

669 6. The combined action of high temperatures (≥20°C) and low infiltration rates (≤0.01

670 m/h) could lead to transient anoxic conditions during future summer conditions. Even

671 under fully anoxic conditions, no complete denitrification was observed, so that nitrate

672 acts as a redox buffer preventing the reductive dissolution of Mn(III/IV)(hydr)oxides.

673 7. Mn(II) was mobilized, whereas Fe(II) was not mobilized in absence of oxygen and

674 nitrate, but Fe(III)-reduction cannot be excluded at actual riverbank filtration systems

675 under these conditions.

676

677

678 **Acknowledgements**

687

688

689 **References**

690 Acuna, V., Wolf, A., Uehlinger, U., Tockner, K., 2008. Temperature dependence of stream

691   benthic respiration in an Alpine river network under global warming. Freshwater Biol. 53

692   (10), 2076-2088.

693 Alexander, M., 1999. Biodegradation and bioremediation. Academic Press, San Diego.

694 Bourg, A.C.M., Bertin, C., 1993. Biogeochemical processes during the infiltration of river water

695   into an alluvial aquifer. Environ. Sci. Technol. 27 (4), 661-666.

696 Brugger, A., Wett, B., Kolar, I., Reitner, B., Herndl, G.J., 2001. Immobilization and bacterial

697   utilization of dissolved organic carbon entering the riparian zone of the alpine Enns

698   River, Austria. Aquat. Microb. Ecol. 24 (2), 129-142.

699 Burdige, D.J., 2011. Temperature dependence of organic matter remineralization in deeply-

700   buried marine sediments. Earth Planet. Sc. Lett. 311 (3-4), 396-410.

701 CH2011, 2011. Swiss Climate Change Scenarios CH2011. C2SM, MeteoSwiss, ETH, NCCR

702   Climate and OcCC, Zurich, pp. 88.

703   Deborde, M., von Gunten, U., 2008. Reactions of chlorine with inorganic and organic

704   compounds during water treatment-Kinetics and mechanisms: A critical review. Water

705   Res. 42 (1-2), 13-51.

706   Diem, S., Cirpka, O.A., Schirmer, M., 2013a. Modeling the dynamics of oxygen consumption

707   upon riverbank filtration by a stochastic-convective approach. J. Hydrol. 505, 352-363.

708   Diem, S., Rudolf von Rohr, M., Hering, J.G., Kohler, H.P.E., Schirmer, M., von Gunten, U.,

709   2013b. NOM degradation during river infiltration: Effects of the climate variables

710   temperature and discharge. Water Res. 47 (17), 6585-6595.

711   DIN, 1983a. Deutsche Einheitsverfahren zur Wasser-, Abwasser- und Schlammuntersuchung,

712   Bestimmung des Ammonium-Stickstoffs (E5), Teil 5, DIN 38406. Deutsches Institut für

713   Normung DIN, pp. 1-6.

714   DIN, 1983b. Deutsche Einheitsverfahren zur Wasser-, Abwasser- und Schlammuntersuchung,

715   Bestimmung von Mangan (E2), Teil 2, DIN 38406. Deutsches Institut für Normung DIN,

716   pp. 1-8.

717   DIN, 1993. Deutsche Norm zur Bestimmung von Nitrit, EN 26777. Deutsches Institut für

718   Normung DIN, pp. 1-11.

719   Doussan, C., Poitevin, G., Ledoux, E., Delay, M., 1997. River bank filtration: Modelling of the

720   changes in water chemistry with emphasis on nitrogen species. J. Contam. Hydrol. 25

721   (1-2), 129-156.

722   Egli, T., 1995. The ecological and physiological significance of the growth of heterotrophic

723   microorganisms with mixtures of substrates. In: Jones, G.N. (Ed.), Advances in

724   Microbial Ecology. Plenum Press, New York, pp. 305-386.

725   EU, 1998. European Union (EU) Council Directive 98/83/EC of 3 November 1998 on the

726   quality of water intended for human consumption.

727   FOEN, 2012. Effects of Climate Change on Water Resources and Watercourses. Synthesis

728   Report on the "Climate Change and Hydrology in Switzerland" (CCHydro) Project.

729   Federal Office for the Environment FOEN, Bern, pp. 76.

730   Green, T.R., Taniguchi, M., Kooi, H., Gurdak, J.J., Allen, D.M., Hiscock, K.M., Treidel, H.,

731   Aureli, A., 2011. Beneath the surface of global change: Impacts of climate change on

732   groundwater. J. Hydrol. 405 (3-4), 532-560.

733   Greskowiak, J., Prommer, H., Massmann, G., Nützmann, G., 2006. Modeling seasonal redox

734   dynamics and the corresponding fate of the pharmaceutical residue phenazone during

735   artificial recharge of groundwater. Environ. Sci. Technol. 40 (21), 6615-6621.

736   Grischek, T., Hiscock, K.M., Metschies, T., Dennis, P.F., Nestler, W., 1998. Factors affecting

737   denitrification during infiltration of river water into a sand and gravel aquifer in Saxony,

738   Germany. Water Res. 32 (2), 450-460.

739   Grünheid, S., Amy, G., Jekel, M., 2005. Removal of bulk dissolved organic carbon (DOC) and

740   trace organic compounds by bank filtration and artificial recharge. Water Res. 39 (14),

741   3219-3228.

742   Grünheid, S., Huebner, U., Jekel, M., 2008. Impact of temperature on biodegradation of bulk

743   and trace organics during soil passage in an indirect reuse system. Water Sci. Technol.

744   57 (7), 987-994.

745   Hannappel, S., Scheibler, F., Huber, A., Sprenger, C., 2014. Characterization of European

746   managed aquifer recharge (MAR) sites - Analysis. EU project Demeau, M11.1, pp 51.

747   Henze, M., Gujer, W., Mino, T., Matsuo, T., Wentzel, M.C., Marais, G.V.R., Van Loosdrecht,

748   M.C.M., 1999. Activated Sludge Model No.2d, ASM2d. Water Sci. Technol. 39 (1), 165-

749   182.

750   Herbert, D., Phipps, P.J., Strange, R.E., 1971. Chemical Analysis of Microbial Cells (Chapter

751   III). In: Methods In Microbiology, Volume 5, Part B. Edited by J.R. Norris and D.W.

752   Ribbons. Academic Press. .

753   Hoehn, E., Scholtis, A., 2011. Exchange between a river and groundwater, assessed with

754   hydrochemical data. Hydrol. Earth Syst. Sc. 15 (3), 983-988.

755   Huntscha, S., Rodriguez Velosa, D.M., Schroth, M.H., Hollender, J., 2013. Degradation of

756   Polar Organic Micropollutants during Riverbank Filtration: Complementary Results from

757   Spatiotemporal Sampling and Push–Pull Tests. Environ. Sci. Technol. 47 (20), 11512-

758   11521.

759   Hyacinthe, C., Bonneville, S., Van Cappellen, P., 2006. Reactive iron(III) in sediments:

760   Chemical versus microbial extractions. Geochim. Cosmochim. Acta 70 (16), 4166-

761   4180.

762   Jacobs, L.A., von Gunten, H.R., Keil, R., Kuslys, M., 1988. Geochemical changes along a

763   river-groundwater infiltration flow path: Glattfelden, Switzerland. Geochim. Cosmochim.

764   Acta 52 (11), 2693-2706.

765   Joss, A., Siegrist, H., Ternes, T.A., 2008. Are we about to upgrade wastewater treatment for

766   removing organic micropollutants? Water Sci. Technol. 57 (2), 251-255.

767   Kedziorek, M.A.M., Geoffriau, S., Bourg, A.C.M., 2008. Organic matter and modeling redox

768   reactions during river bank filtration in an alluvial aquifer of the Lot River, France.

769   Environ. Sci. Technol. 42 (8), 2793-2798.

770   Kuehn, W., Mueller, U., 2000. Riverbank filtration: An overview. J. Am. Water Works Ass. 92

771   (12), 60-69.

772   Kunz, Y., von Gunten, U., Maurer, M., 2009. Wasserversorgung 2025 - Vorprojekt. Eawag, pp.

773   198.

774   Maeng, S.K., Sharma, S.K., Magic-Knezev, A., Amy, G., 2008. Fate of effluent organic matter

775   (EfOM) and natural organic matter (NOM) through riverbank filtration. Water Sci.

776   Technol. 57 (12), 1999-2007.

777   Massmann, G., Greskowiak, J., Dunnbier, U., Zuehlke, S., Knappe, A., Pekdeger, A., 2006.

778   The impact of variable temperatures on the redox conditions and the behaviour of

779   pharmaceutical residues during artificial recharge. J. Hydrol. 328 (1-2), 141-156.

780   Matsunaga, T., Karametaxas, G., von Gunten, H.R., Lichtner, P.C., 1993. Redox chemistry of

781   iron and manganese minerals in river-recharged aquifers: A model interpretation of a

782   column experiment. Geochim. Cosmochim. Acta 57 (8), 1691-1704.

783 Middelburg, J.J., Klaver, G., Nieuwenhuize, J., Wielemaker, A., De Haas, W., Vlug, T., Van

784   Der Nat, J.F.W.A., 1996. Organic matter mineralization in intertidal sediments along an

785   estuarine gradient. Mar. Ecol.-Prog. Ser. 132 (1-3), 157-168.

786 Mouchet, P., 1992. From conventional to biological removal of iron and manganese in France.

787   J. Am. Water Works Ass. 84 (4), 158-167.

788 Mueller, B., 2004. ChemEQL, V.3.0, a program to calculate chemical speciation and chemical

789   equilibria, Eawag.

790 Müller, R., Widemann, O., 1955. Die Bestimmung des Nitrat-Ions im Wasser. Vom Wasser 22,

791   247-271.

792 Nowotny, N., Epp, B., von Sonntag, C., Fahlenkamp, H., 2007. Quantification and modeling of

793   the elimination behavior of ecologically problematic wastewater micropollutants by

794   adsorption on powdered and granulated activated carbon. Environ. Sci. Technol. 41

795   (6), 2050-2055.

796 O'Connell, A.M., 1990. Microbial decomposition (respiration) of litter in eucalypt forests of

797   South-Western Australia: An empirical model based on laboratory incubations. Soil

798   Biol. Biochem. 22 (2), 153-160.

799 OECD, 1992. OECD Guideline for Testing of Chemicals, Guideline 301 D. Organisation for

800   Economic Co-operation and Development OECD pp. 62.

801 Peter, S., Koetzsch, S., Traber, J., Bernasconi, S.M., Wehrli, B., Durisch-Kaiser, E., 2012.

802   Intensified organic carbon dynamics in the ground water of a restored riparian zone.

803   Freshwater Biol. 57 (8), 1603-1616.

804 Pusch, M., Fiebig, I., Brettar, H., Eisenmann, H., Ellis, B.K., Kaplan, L.A., Lock, M.A., Naegeli,

805   M.W., Traunspurger, W., 1998. The role of micro-organisms in the ecological

806   connectivity of running waters. Freshwater Biol. 40 (3), 453-495.

807 Scheurer, M., Michel, A., Brauch, H.J., Ruck, W., Sacher, F., 2012. Occurrence and fate of the

808   antidiabetic drug metformin and its metabolite guanylurea in the environment and

809   during drinking water treatment. Water Res. 46 (15), 4790-4802.

810 Schmidt, C.K., Lange, F.T., Brauch, H.J., 2007. Characteristics and evaluation of natural

811   attenuation processes for organic micropollutant removal during riverbank filtration.

812   Wat. Sci. Technol. 7 (3), 1-7.

813 Schoenheinz, D., Grischek, T., 2011. Behavior of dissolved organic Carbon during bank

814   filtration under extreme climate conditions. NATO Science for Peace and Security

815   Series C: Environmental Security 103, 51-67.

816 Smith, P.K., Krohn, R.I., Hermanson, G.T., 1985. Measurement of protein using bicinchoninic

817   acid. Anal. Biochem. 150 (1), 76-85.

818 Sobczak, W.V., Findlay, S., 2002. Variation in bioavailability of dissolved organic carbon

819   among stream hyporheic flowpaths. Ecology 83 (11), 3194-3209.

820 Sprenger, C., Lorenzen, G., Hulshoff, I., Grutzmacher, G., Ronghang, M., Pekdeger, A., 2011.

821   Vulnerability of bank filtration systems to climate change. Sci. Total Environ. 409 (4),

822   655-663.

823 Storck, F.R., Schmidt, C.K., Wülser, R., Brauch, H.J., 2012. Effects of boundary conditions on

824   the cleaning efficiency of riverbank filtration and artificial groundwater recharge

825   systems regarding bulk parameters and trace pollutants. Water Sci. Technol. 66 (1),

826   138-144.

827 Stumm, W., Morgan, J.J., 1996. Aquatic Chemistry. Chemical Equilibria and Rates in Natural

828   Waters, Third Edition. Wiley-interscience, New York.

829 Tufenkji, N., Ryan, J.N., Elimelech, M., 2002. Bank filtration. Environ. Sci. Technol. 36 (21),

830   423-428.

831 Valentini, A., Garuti, G., Rozzi, A., Tilche, A., 1997. Anaerobic degradation kinetics of

832   particulate organic matter: A new approach. Water Sci. Technol. 36 (6-7), 239-246.

833 Vavilin, V.A., Fernandez, B., Palatsi, J., Flotats, X., 2008. Hydrolysis kinetics in anaerobic

834   degradation of particulate organic material: An overview. Waste Management 28 (6),

835   939-951.

836 Vogler, P., 1965. Beiträge zur Phosphatanalytik in der Limnologie. II. Die Bestimmung des

837   gelösten Ortophosphates. Fortschritte der Wasserchemie und ihrer Grenzgebiete 2,

838   109-119.

839 von Gunten, H.R., Karametaxas, G., Krähenbühl, U., Kuslys, M., Giovanoli, R., Hoehn, E., Keil,

840   R., 1991. Seasonal biogeochemical cycles in riverborne groundwater. Geochim.

841   Cosmochim. Acta 55 (12), 3597-3609.

842 von Gunten, U., Zobrist, J., 1993. Biogeochemical changes in groundwater-infiltration systems:

843   Column studies. Geochim. Cosmochim. Acta 57 (16), 3895-3906.

844 Weston, N.B., Joye, S.B., 2005. Temperature-driven decoupling of key phases of organic

845   matter degradation in marine sediments. P. Natl. Acad. Sci. USA 102 (47), 17036-

846   17040.

847 WHO, 2011. Guidelines for Drinking-water Quality, Fourth Edition. World Health Organization

848   WHO, pp. 541.

849 Worch, E., 2010. Competitive adsorption of micropollutants and NOM onto activated carbon:

850   Comparison of different model approaches. J. Water Supply Res. T. 59 (5), 285-297.

851 Zimmermann, S.G., Wittenwiler, M., Hollender, J., Krauss, M., Ort, C., Siegrist, H., von

852   Gunten, U., 2011. Kinetic assessment and modeling of an ozonation step for full-scale

853   municipal wastewater treatment: Micropollutant oxidation, by-product formation and

854   disinfection. Water Res. 45 (2), 605-617.

855

856

857

858

859

860

861

862

863

Figure captions

Fig. 1. (a) Profiles of the relative oxygen concentration (normalized to the values at SP0) and (b) pH for "DOM-free" Thur River water (n=3) (○), Thur River water (n=1) (◆), Thur River water/effluent mixtures (*average of four mixtures: 90/10, 80/20, 70/30, 60/40%) (□) and Thur River water amended with 1.75 mg C/L sodium acetate (n=3) (△). The first data point corresponds to the sampling port at the inlet (SP0), the last data point to the sampling port at the outlet of the column (SP14) for each experiment. Mean values and standard deviations are shown as symbols and error bars, respectively.

Fig. 2. Net biological oxygen demand (BOD) of the pristine sand (mg oxygen/mg sand) determined in individual batch experiments conducted for 5, 7, 14, 21 and 28 days. Mean values (n=2) are shown corrected for the blank associated with oxygen uptake by the inoculum; Error of measurement is $<1 \times 10^{-5}$ mg O_2 / mg sand.

Fig. 3. Profiles of the relative oxygen concentration (normalized to the values at SP1) as a function of (a) infiltration distance and (b) residence time at flow rates of 0.10 (n=1), 0.20 (n=1), 0.33 (n=1) and 1.00 (n=13) mL/min at 20°C. Mean values and standard deviations (for 1 mL/min) are shown as symbols and error bars, respectively.

Fig. 4. Total average oxygen and DOM (as DOC) consumption in column experiments between SP0 and SP14. Standard deviations are shown as error bars (n=3).

Fig. 5. Measured oxygen concentration profiles (symbols) and least-squares linear regression lines at 5.0, 12.5, 20.0 and 30.0°C at a flow rate of 0.3 mL/min. Mean

889   values and standard deviations are shown as symbols and error bars, respectively

890   (n=3).

891

892   Fig. 6. Schematic representation of oxygen consumption associated with degradation

893   of POM on sand grains. Reaction (1) represents POM hydrolysis and reaction (2)

894   BDOM oxidation.

895

896   Fig. 7. Protein concentration (expressed as bovine serum albumin concentration, BSA)

897   of the sand from column II (SP1, SP2, SP3, SP5, SP8, SP9, SP10, SP11, SP12,

898   SP13) (●) measured after 393 days of operation (Table 2, end of experiment 2.5) and

899   of pristine sand (dashed line). The dotted lines represent the errors of measurement

900   for the pristine sand (n=3). Mean values and standard deviations are shown as

901   symbols and error bars, respectively (n=3).

902

903   Fig. 8. Arrhenius-type correlation between the rate constant ($\ln(k)$) for oxygen

904   consumption and $\frac{1}{T}$. The symbols represent the experimental data at 30.0, 20.0, 12.5

905   and 5.0°C (n=3) (Fig. 5), the line shows a least-squares linear regression.

906

907   Fig. 9. Measured oxygen (- - -), nitrate (◇), nitrite (△) and ammonium (●) concentrations

908   after 18 days of operation of column II at 30.0°C at a flow rate of 0.3 mL/min (Table 2,

909   experiment 2.1). Mean values and standard deviations (for nitrate) are shown as

910   symbols and error bars, respectively (n=3). For nitrate, nitrite and ammonium, lines

911   help to guide the reader's eye.

912

913   Fig. 10. (a) Mn(II) concentration at SP0 (●), SP1 (○), SP5 (▼), SP8 (△), SP11 (■) and

914   SP14 (□) as a function of the column operation time at 20°C and at a flow rate of 0.3

915   mL/min. The Mn(II) concentration in equilibrium with rhodochrosite ($MnCO_3$) is shown

916   by the dashed line (for calculations, see Section 2.4). (b) Average amount of Mn

917   reduced [µg/g sand] by ascorbate in the pristine (dashed line) and in the sand from

918   column II (circles) (SP1, SP5, SP8, SP11 and SP13) after 66 days of operation. For

919   the pristine sand, an average of three samples after 0.5, 1, and 2.5 hours equilibration

920   with the ascorbate solution is shown with the errors of measurement (dotted lines), for

921   the column II samples, an average of samples after 0.5, 1, and 2.5 hours equilibration

922   is shown together with the corresponding standard deviations.

Table 1. Hydraulic characteristics of the columns (effective porosity, dispersivity and total pore volume) and sand mass present in the columns. The effective porosity and the dispersivity were calculated with the program CXTFIT (Toride et al., 1995) using the electrical conductivity data.

	Column I	Column II
Effective porosity [-]	0.38	0.32
Dispersivity [cm]	0.1	0.1
Total pore volume [mL]	245	206
Sand mass [g]	885	876

Table 2. Operational conditions of all column experiments, which are listed in a chronological order for columns I (1.1, 1.2) and II (2.1-2.5). Experiments 1.2, 2.1 and 2.2 were conducted with unaltered Thur River water as feed water.

Experiment	Flow rate [mL/min] ([m/h])	Residence time [h]	Temperature [°C]	Column
(1.1) Thur River water/effluent mixtures[a]	1.0 (0.07)	4	22	I
(1.2) Variation of flow rate	0.1 (0.007), 0.2 (0.01)	40, 20	20	I
	0.33 (0.02), 1.0 (0.07)	12, 4		
(2.1) Variation of temperature	0.3 (0.03)	11.5	5, 12.5, 20, 30	II
(2.2) Thur River water	0.3 (0.03)	11.5	20	II
(2.3) Addition of "DOM-free" Thur River water	0.3 (0.03)	11.5	20	II
(2.4) Addition of acetate	1.0 (0.09)	3.5	20	II
(2.5) Addition of oxygen- and nitrate-free Thur River water	0.3 (0.03)	11.5	20	II

[a] 90/10, 80/20, 70/30, 60/40%

	Aqueous solution
O_2 CO_2	
$BDOM + O_2 \xrightarrow{(2)} CO_2 + H_2O$	Biofilm
(1)	
POM	POM coating
	Sand grain

Mn equilibrium

SP11 (a)

SP14

SP8

SP5

SP1

SP0

Mn concentration [µg/L]

Time after starting experiment [days]

pristine sand (b)

SP11

SP8

SP5

SP1

SP13

Amount Mn reduced [µg/g]

sand column II

Column distance [cm]